Collimating Three-Axicon Zoom System for Interferometric Bessel Beam Side Lobe Cancellation

Optical and Quantum Electronics

Marco Schnieder[1,2*], Anna Niemann[1,2], Jana Hüve[1,2*†], Jürgen Klingauf[1,2*†]

[1]Fluorescence Microscopy Facility Münster (FM)², Institute of Medical Physics and Biophysics, University of Münster, 48149 Münster, Germany.
[2]Institute of Medical Physics and Biophysics, University of Münster, Robert-Koch-Straße 31, 48149 Münster, Germany.

*Corresponding author(s). E-mail(s): ma.schnieder@uni-muenster.de; jana.hueve@uni-muenster.de; klingauf@uni-muenster.de;
Contributing authors: a_niem08@uni-muenster.de;
†Jana Hüve and Jürgen Klingauf contributed equally to this work.

Supplementary Information

1 Properties of the SWAN System Derived by Geometrical Optics

With the ABCD matrices for lenses and beam propagation as well as the function F for axicons

$$\underline{\mathbf{L}} = \begin{pmatrix} 1 & 0 \\ -\frac{1}{f} & 1 \end{pmatrix}, \quad \underline{\mathbf{D}} = \begin{pmatrix} 1 & d \\ 0 & 1 \end{pmatrix}, \quad F\left(\begin{pmatrix} y \\ \theta \end{pmatrix}; \alpha, n\right) = \begin{cases} \begin{pmatrix} y \\ \alpha(1-n)+\theta \end{pmatrix} & \text{for} \quad y > 0 \\ \begin{pmatrix} y \\ \alpha(n-1)+\theta \end{pmatrix} & \text{for} \quad y < 0, \end{cases}$$

it can be derived why the general configuration of the optical elements belonging to the SWAN system (cf. Supplementary Fig. 1) has to be adjusted as indicated in Fig. 1 in the main text in order to get a collimated ring intensity out of the system.

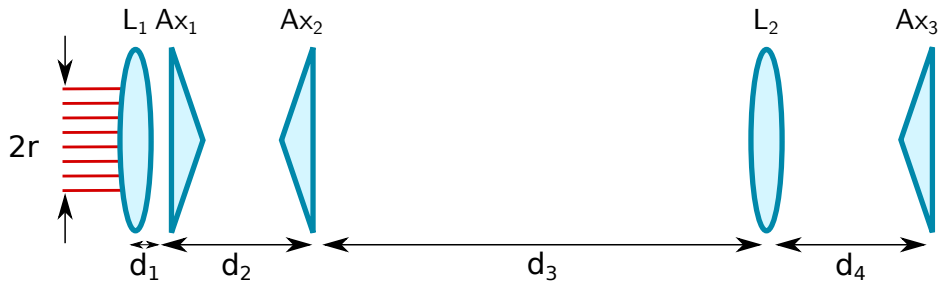

Fig. 1 Sketch of the SWAN setup's elements without presumptions on how to adjust the elements.

As a starting point, according to the function F, an axicon adds an angle $\pm\alpha(n-1)$ to the incident beam depending on if it hits the axicon above or below the cone's tip. If the beam

$$\begin{pmatrix} y_1 \\ \theta_1 \end{pmatrix} = \underline{\mathbf{D}}(d_1)\underline{\mathbf{L}}(f_1) \begin{pmatrix} y_{\text{in}} \\ \theta_{\text{in}} \end{pmatrix} \tag{1}$$

incident on the first axicon Ax_1 propagates such that y_2, defined by

$$\begin{pmatrix} y_2 \\ \theta_2 \end{pmatrix} = \underline{\mathbf{D}}(d_2) F \left(\begin{pmatrix} y_1 \\ \theta_1 \end{pmatrix}; \alpha, n \right) = \begin{pmatrix} y_1 + d_2(\pm\alpha(1-n) + \theta_1) \\ \pm\alpha(1-n) + \theta_1 \end{pmatrix}, \tag{2}$$

changes its sign with respect to y_1, then the second axicon Ax_2 is going to remove the added angle introduced by the first axicon. In this special case, the beam directly behind Ax_2 is given by

$$\begin{pmatrix} y_3 \\ \theta_3 \end{pmatrix} = F \left(\begin{pmatrix} y_2 \\ \theta_2 \end{pmatrix}; \alpha, n \right) \overset{(2)}{=} \begin{pmatrix} y_1 + d_2(\pm\alpha(1-n) + \theta_1) \\ \theta_1 \end{pmatrix}. \tag{3}$$

The validity of assuming the sign change in y can be estimated via an equation for the distance L at which an incident collimated beam at height y crosses the optical axis (Wang et al (2017)):

$$L = y\tan\gamma - y\tan\alpha \quad \text{where} \quad \gamma = \frac{\pi}{2} - \beta + \alpha,\ \sin\beta = n\sin\alpha \tag{4}$$

Inserting exemplary values of $\alpha = 10°$, $n = 1.46$ into equation (4) shows that for having $\text{L} \leq 10\,\text{cm}$, the incident beam radius should not exceed 8.3 mm so that the beam may be expanded, but not fill the whole aperture of e.g. 2.54 cm. This demonstrates that the assumption that y has to change its sign requires some attention in the experimental design, but can be fulfilled with reasonable effort.

The complete SWAN system is represented by

$$\begin{aligned}\begin{pmatrix} y_{\text{out}} \\ \theta_{\text{out}} \end{pmatrix} &= F\left(\underline{\mathbf{D}}(d_4)\underline{\mathbf{L}}(f_2)\underline{\mathbf{D}}(d_3)\begin{pmatrix} y_3 \\ \theta_3 \end{pmatrix}; \alpha, n\right) \\ &= \begin{pmatrix} \left(1-\frac{d_4}{f_2}\right) y_3 + \left(d_3 + (1-\frac{d_3}{f_2})d_4\right)\theta_3 \\ \pm\alpha(1-n) - \frac{y_3}{f_2} + (1-\frac{d_3}{f_2})\theta_3 \end{pmatrix}.\end{aligned} \tag{5}$$

Equation (5) describes a collimated beam if the angle-related term disappears independent of the incidence height y_{in}. For checking the possibility to create collimated beams, equations (1) to (3) are inserted into equation (5). The full dependence of the output angle θ_{out} is thus written as

$$\theta_{\text{out}} = \pm\alpha(1-n)\left(1-\frac{d_2}{f_2}\right) + y_{\text{in}}\left(\frac{d_1+d_2+d_3-f_1-f_2}{f_1 f_2}\right) + \theta_{\text{in}}\left(1-\frac{d_2+d_3}{f_2}\right). \tag{6}$$

The first term of equation (6) disappears for a distance $d_2 = f_2$ between the first two axicons whereas the second term disappears if the two lenses are adjusted to a $4f$ configuration. The last term does not disappear for all incidence angles θ_{in}. If $\theta_{\text{in}} = 0$, though, θ_{out} will also vanish.

Having derived these requirements for adjustment, the output radius r of the collimated beam can be calculated as

$$\begin{aligned} r &= \begin{pmatrix} y_{\text{out}} \\ \theta_{\text{out}} \end{pmatrix}(y_{\text{in}}, \theta_{\text{in}}) - \begin{pmatrix} y_{\text{out}} \\ \theta_{\text{out}} \end{pmatrix}(0, \theta_{\text{in}}) \\ &\overset{(5)}{=} y_{\text{in}}\left(1 - \frac{d_1+d_2+d_3+d_4}{f_1} - \frac{d_4}{f_2} + \frac{(d_1+d_2+d_3)d_4}{f_1 f_2}\right) \overset{d_2=f_2,\ d_3=f_1-d_1}{=} -\frac{f_2}{f_1} y_{\text{in}}\end{aligned} \tag{7}$$

This means that besides collimation, the SWAN system behaves like a telescope as it diminishes the output ring radius by a factor of $-f_2/f_1$.

2 Calculation of Strongly Focused Fields

The theory of how to calculate focused fields has been thoroughly developed before (Foreman and Török (2011); Novotny and Hecht (2012)) so that here we will mostly only mention the equations we used for predicting the field distributions. As in this study, the influence of azimuthal modulation upon interference patterns was of interest, however, we will present an approximation for ϕ-dependent fields which is usually not considered.

If an arbitrarily polarized field

$$\vec{E}_{\text{inc}} = E_{\text{inc}}(\Theta, \Phi)\begin{pmatrix} \tilde{E}_x \\ \tilde{E}_y \\ 0 \end{pmatrix} \tag{8}$$

with $\tilde{E}_x$, $\tilde{E}_y$ being the Jones vector components falls onto a focusing lens, the field is projected onto a Gaussian reference sphere. This case has been discussed by Foreman and Török (2011). For a transition from a medium with refractive index n_1 in front of the lens to a medium with n_2 behind the lens, the projected field $\vec{e}$ reads

$$\vec{e}(\Theta,\Phi) = \left(t^s(\vec{E}_{\text{inc}}\cdot\vec{n}_\Phi)\vec{n}_\Phi + t^p(\vec{E}_{\text{inc}}\cdot\vec{n}_\rho)\vec{n}_\Theta\right)\sqrt{\frac{n_1}{n_2}\cos(\Theta)} \tag{9}$$

where t^s, t^p are the transmission coefficients for perpendicular and parallel polarized light, respectively, and $\vec{n}_{\rho,\Theta,\Phi}$ the normal vectors for spherical coordinates. Inserting equation (8) into equation (9) results in

$$\begin{aligned}\vec{e}(\Theta,\Phi) =& \frac{1}{2}\sqrt{\frac{n_1}{n_2}\cos(\Theta)}E_{\text{inc}}(\Theta,\Phi)\times \\ & \begin{pmatrix} \tilde{E}_x[(1+\cos(\Theta))+(\cos(\Theta)-1)\cos(2\Phi)] + \tilde{E}_y(\cos(\Theta)-1)\sin(2\Phi) \\ \tilde{E}_x(\cos(\Theta)-1)\sin(2\Phi) + \tilde{E}_y[(1+\cos(\Theta))-(\cos(\Theta)-1)\cos(2\Phi)] \\ -2\sin(\Theta)(\tilde{E}_x\cos(\Phi)+\tilde{E}_y\sin(\Phi)) \end{pmatrix}.\end{aligned} \tag{10}$$

With the help of the angular spectrum representation and the method of stationary phase, the analytic expression for the focal field $\vec{E}$ is

$$\vec{E}(\rho,\phi,z) = \frac{\mathrm{i}kf\mathrm{e}^{-\mathrm{i}kf}}{2\pi}\int_0^{\Theta_{\max}}\int_0^{2\pi}\vec{e}(\Theta,\Phi)\mathrm{e}^{\mathrm{i}kz\cos(\Theta)}\mathrm{e}^{\mathrm{i}k\rho\sin(\Theta)\cos(\Phi-\phi)}\sin(\Theta)d\Phi d\Theta \tag{11}$$

where f is the focusing lens' focal length, k the wave number and z the axial distance from the lens' focal plane.

2.1 Radially Symmetric Fields

Numerically, equation (11) can be solved via integration for arbitrary incident fields. Due to two integrals being present and small angular step widths being necessary to resolve the complex phases, this is not time-efficient, though. If the incident field $\vec{E}_{\text{inc}}(\Theta,\Phi) = \vec{E}_{\text{inc}}(\Theta)$ is radially symmetric, the azimuthal integral in equation (11) can be solved using the relations

$$\begin{aligned}\int_0^{2\pi}\cos(n\Phi)\mathrm{e}^{\mathrm{i}x\cos(\Phi-\phi)}d\Phi &= 2\pi(\mathrm{i}^n)J_n(x)\cos(n\phi) \\ \int_0^{2\pi}\sin(n\Phi)\mathrm{e}^{\mathrm{i}x\cos(\Phi-\phi)}d\Phi &= 2\pi(\mathrm{i}^n)J_n(x)\sin(n\phi)\end{aligned} \tag{12}$$

In this case, only the integrals over Θ remain and the solution can be written down in terms of these (Foreman and Török (2011); Novotny and Hecht (2012)). The intensity

pattern shown in Figure 2c) in the main text has been calculated like this and by taking $|\vec{E}(\rho, \phi, 0)|^2$ as the expected intensity.

2.2 Infinitesimally Thin Fields with Azimuthal Dependence

The Bessel beam (BB) of 1st kind and 0th order has got a central core surrounded by theoretically an infinite number of side lobes. The first side lobes can be significantly reduced by interfering two BBs with different k-vectors which at the same time introduces axial interference. For this reason, this approach has been baptised "droplet beams" (Antonacci et al (2017)). If this axial interference shall be avoided, another option for destructive interference has been theoretically proposed in the context of STED microscopy (Zhang et al (2014)): from Debye diffraction theory, it has been derived that the superposition of a J_0 and a J_2 BB leads to destructively interfering side lobes in one lateral direction.

For similar considerations in the vectorial theory sketched above, we assume now that the incident field has got the form

$$\vec{E}_{\mathrm{inc}}(\Theta, \Phi) = \delta(\Theta - \Theta_0)\mathcal{E}(f, f\sin(\Theta), \Phi) \begin{pmatrix} \tilde{E}_x \\ \tilde{E}_y \\ 0 \end{pmatrix} \tag{13}$$

which corresponds to an infinitesimally thin annular field with azimuthal dependence. The δ-distribution appearing in equation (13) projects equation (11) onto the integral over Φ which can be solved numerically. This means that the exponential $\exp(ikz\cos(\Theta))$ is drawn out of the integral and that the intensity $|\vec{E}|^2$ does not have any axial dependence any more. This is expected as an infinitesimally thin incident annular field corresponds to a non-diffracting field.

3 Cancellation of Bessel Beam Side Lobes without Tuneable Parameters

The combination of the SWAN system and a Michelson interferometer allows for interferometric cancellation of BB side lobes and choosing the effective numerical aperture (NA) that determines the lateral dimensions of the BB. For some applications, a single well-defined effective NA is sufficient so that a simplified optical system can be used.

In the following, we theoretically discuss the generation of interfering BBs with the help of a Michelson interferometer that is illuminated with a Gaussian input beam. Generally, also other interferometer types as a Mach-Zehnder interferometer are theoretically suited to generate destructive interference of BB side lobes in one direction. For the case of a Mach-Zehnder interferometer, suitable phase plates could be introduced to manipulate the fields accordingly. We restrict the discussion to the Michelson interferometer, though, because this is the interferometer we also used experimentally. Simplifying the generation of BB, the idea is to convert the interfered field by a single axicon as sketched in Fig. 2a).

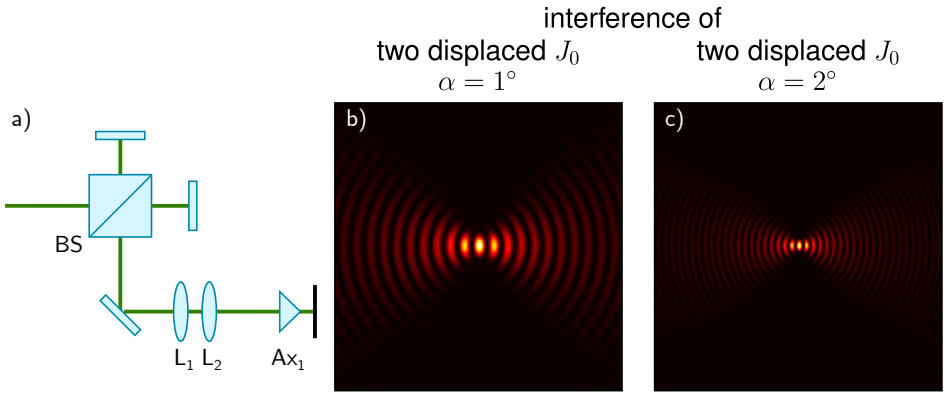

Fig. 2 a) Simplified optical system consisting of a Michelson interferometer, lenses and a single axicon. Behind the beam splitter (BS), two lenses L_1, L_2 are used to image the mirror planes onto the back of axicon Ax_1. The apex angle of Ax_1 determines the BB's size so that e.g. b) an angle of $\alpha = 1°$ will generate a larger BB than c) an angle of $\alpha = 2°$.

For the numerical calculation of the expected field, the vectorial description presented in section 2 is not suited because it assumes the projection on a reference sphere, i.e. focusing by a lens. The setup sketched in Fig. 2 a) generates the BB with a single axicon so that we calculated the field as a scalar field U in terms of Fourier optics. The calculation method is described in detail by Goodman (2017).

For calculating the interfering field $U = U_1 + U_2$ in the observation plane (black line in Fig. 2 a)), we assumed a Gaussian input field as described in chapter 4.6.1 of Goodman (2017). For demonstration, we choose an expanded Gaussian beam with $w_0 = 3.5\,\mathrm{mm}$, a divergence angle $\theta_0 = 1.2\,\mathrm{mrad}$ and wavelength $\lambda = 561\,\mathrm{nm}$. These parameters correspond to values that would be expected in our experiments. We set $z_1 = z_2 = 10\,\mathrm{cm}$.

It is necessary to image the interferometer's mirror planes onto the back aperture of the axicon in order to convert a tilt of one mirror into a change of the incident angle on the axicon without displacing the beam. We assume that in front of the axicon, $U_{1,in}$ stays a Gaussian field without change whereas $U_{2,in}$ gathers a phase factor $\exp(i\pi \sin(\phi))$ corresponding to a slight tilt of the mirror. The field U_{out} directly behind the axicon is given by

$$U_{out} = \left(U_{1,in} + U_{2,in} e^{i\pi \sin(\phi)}\right) e^{-ik(n-1)\rho\alpha} \tag{14}$$

where the phase factor introduced by the axicon (Wang et al, 2017) is dependent on the wave number k, the refractive index n, the apex angle α and the polar radius ρ. Here, we assumed a refractive index $n = 1.46$.

In Fourier optics, the propagation of the field is calculated by applying a Fourier transformation $\mathcal{F}$ to the field and multiplying a transfer function $H(f_X, f_Y)$ where f_X, f_Y are spatial frequencies. The propagated field in real space is finally obtained

by inverse Fourier transformation $\mathcal{F}^{-1}$:

$$U = \mathcal{F}^{-1}\left(\mathcal{F}\left(U_{out}\right) \cdot \underbrace{e^{ikz} e^{-i\pi\lambda z_{prop}\left(f_X^2+f_Y^2\right)}}_{H(f_X,f_Y)}\right) \tag{15}$$

Using these equations, we calculated U for two different apex angles $\alpha = 1°$, $2°$ and present the BBs expected after a propagation length of $z_{prop} = 12\,\mathrm{cm}$ in Fig. 2 b) and c). Qualitatively, two observations are important: Firstly, the numerical calculation suggests that the uni-axial cancellation of BB side lobes is expected in this simpler optical setup. Secondly, the fields generated by the two different apex angles illustrate that a higher apex angle α corresponds to smaller lateral parameters of the BB.

References

Antonacci G, Domenico G, Silvestri S, et al (2017) Diffraction-free light droplets for axially-resolved volume imaging. Scientific Reports 7(1):1–6. https://doi.org/10.1038/s41598-017-00042-w

Foreman M, Török P (2011) Computational methods in vectorial imaging. Journal of Modern Optics 58(5-6):339–364. https://doi.org/10.1080/09500340.2010.525668

Goodman J (2017) Introduction to Fourier Optics, 4th edn. Macmillan Learning, New York, USA, Chapters 3-5

Novotny L, Hecht B (2012) Principles of Nano-Optics, 2nd edn. Cambridge University Press, Cambridge, United Kingdom, https://doi.org/10.1017/CBO9780511794193, Chapter 3

Wang Y, Yan S, Friberg A, et al (2017) Electromagnetic diffraction theory of refractive axicon lenses. J Opt Soc Am A 34(7):1201–1211. https://doi.org/10.1364/JOSAA.34.001201

Zhang P, Goodwin P, Werner J (2014) Fast, super resolution imaging via Bessel-beam stimulated emission depletion microscopy. Optics Express 22(10):12398–12409. https://doi.org/10.1364/OE.22.012398